Lactoferrin alleviates Western diet-induced cognitive impairment through the microbiome-gut-brain axis

Qian He
Department of Nutrition and Food Hygiene, School of Public Health, Soochow University
Jiangxue Wu
Department of Nutrition and Food Hygiene, School of Public Health, Soochow University
Deming Li
Department of Nutrition and Food Hygiene, School of Public Health, Soochow University
Ya-Xin Guo
Department of Nutrition and Food Hygiene, School of Public Health, Soochow University
Jingbo Fan
Department of Nutrition and Food Hygiene, School of Public Health, Soochow University
Qingyang Wu
School of Life Science The Chinese University of Hong Kong
Hai-Peng Wang
Department of Cardiovascular, The First Affiliated Hospital of Soochow University
Zhongxiao Wan
Department of Nutrition and Food Hygiene, School of Public Health, Soochow University
Jia-Ying Xu
State Key Laboratory of Radiation Medicine and Protection, School of Radiation Medicine and Protection, Soochow University
Li-Qiang Qin (qinliqiang@suda.edu.cn)
Department of Nutrition and Food Hygiene, School of Public Health, Soochow University

Research Article

Keywords: Lactoferrin, 'Western'-style diets, Neuroinflammation, Cognitive impairment, Behavioral change, Hippocampus, Gut microbiota, Microbiome-gut-brain axis

Posted Date: November 17th, 2022

DOI: https://doi.org/10.21203/rs.3.rs-2229442/v1

Abstract

Lactoferrin (Lf) is a multifunctional glycoprotein that showed demonstrated a beneficial effect on cognitive function in several mouse models; however, its mechanisms are not fully elucidated. This study investigated whether Lf improves high-energy-dense 'Western'-style diets (WD)-induced cognitive impairment and neuroinflammation through microbiome-gut-brain axis. Male C57BL/6J mice were randomly divided into the CON, WD, Lf, and Lf+AB groups. The mice in the latter three groups fed with WD. The Lf group was intragastrically administered with Lf and the Lf+AB group additionally drank a solution with antibiotics. Some of the mice in the CON, WD, and Lf groups were killed at 2 weeks. The experiments ended at 16 weeks. Behavioral tests, neuroinflammation, and gut microbiota were analyzed. WD resulted in neuroinflammation and impaired cognition. Lf improved the cognitive function as indicated by behavioral tests including nesting behavior test, novel object recognition test, and the Morris water maze test. It also increased the length and curvature of postsynaptic density as observed with a transmission electron microscope and upregulated the related protein expression, suggesting the improvement of the hippocampal neurons and synapses. Lf suppressed microglia activation and proliferation as revealed by immunofluorescence analysis. It decreased the serum levels of pro-inflammatory cytokines and downregulated their protein expressions in the hippocampus region. Lf also inhibited the activation of NF-κB/NLRP3 inflammasomes in the hippocampus. Meanwhile, WD impaired gut permeability and induced gut dysbiosis. Lf upregulated the expression of tight junction proteins, and increased the abundance of Bacteroidetes at phylum and Roseburia at genus, bothare beneficial for anti-obesity, gut barrier, and cognitive function. The antibiotics supplemented in the Lf+AB group eliminated the effects of long-term Lf intervention on cognitive impairment, suggesting that gut microbiota participated in Lf action. The 2-week Lf intervention prevented WD-induced gut microbiota alteration without inducing behavioral changes; these findings supported the timing sequence of gut microbiota to the brain. In Conclusion, our findings demonstrated that Lf intervention alleviated cognitive impairment by inhibiting microglial activation and neuroinflammation through the microbiome-gut-brain axis.

1. Introduction

High-energy-dense 'Western–style diets (WD) enriched with fat and simple carbohydrates contribute to obesity and obesity-related chronic diseases [1]. WD-induced obesity is also a risk factor for neurodegenerative diseases, such as Alzheimer’s disease (AD) and Parkinson’s disease (PD) [2]. Chronic inflammation is one mechanism linked to obesity-related diseases, including neurodegenerative diseases. Microglia are the resident immune cells of the brain, and their activation induces the secretion of pro-inflammatory factors and then hippocampal inflammation [3]. Neuroinflammation is proposed to be an important pathophysiological hallmark underlying these diseases [4]. Thus, neuroinflammation improvement is an optional way to prevent cognitive impairment.

Stable gut microbiota composition is critical in sustaining the balance of intestinal barrier integrity and inflammation, and thus positively regulating brain development and behavior through the microbiome-gut-brain axis [5, 6]. Many pathological alterations of microbial taxon abundances have been reported in

AD patients. For example, gut dysbiosis may promote amyloid-beta aggregation, neuroinflammation, and oxidative stress in the pathogenesis of AD [7]. Transferring the microbiota of AD patients to amyloid precursor protein (APP)/presenilin-1 (APP/PS1) mice can promote microglia activation and inflammatory response in the hippocampus, further aggravating the pathological progression of AD and leading to declined cognitive and behavioral abilities [8]. Therefore, microbial alteration is involved in neuroinflammation and cognitive impairment [9].

These neurodegenerative diseases are currently not curable; however, the Lancet commission reported that more than one-third of cases may be prevented by addressing lifestyle factors, including diet [10]. Increasing evidence shows that diets can influence the gut microbiome, potentially modulating brain functions through the gut-brain axis. Lactoferrin (Lf) is a component of whey protein and possesses multiple functions, such as anti-inflammatory, antibacterial, reactive oxygen species (ROS) modulator, antiviral, and antitumor immunity effects [11]. A population-based study found that salivary Lf is associated with cortical amyloid-beta load, cortical integrity, and memory in aging [12]. Lf administration could improve the cognitive function of AD patients by affecting key inflammatory and oxidative stress [13]. Lf was detected in senile plaques and neurofibrillary tangles (NFTs) from APP transgenic (APP-Tg) mice [14] and AD patients [13]. Several animal models were used to investigate the effect of Lf administration on cognitive function. Lf and hydrolyzed Lf attenuated memory impairment by inhibiting the amyloidogenic processing of APP in APP-Tg mice [15]. Similarly, intranasal Lf administration improved cognitive function in APP/PS1 mice [14]. However, our previous study found that Lf had no effects on cognitive function but benefited gut microbiota homeostasis in young and middle-aged APP/PS1 mice [16]. Thus, the relationship between Lf and cognitive impairment, and the involved mechanisms are not fully elucidated.

This study aimed to investigate whether Lf alleviates cognitive impairment through neuroinflammation and gut microbiota in obese mice fed WD for 16 weeks. Cognitive function was measured by behavioral tests. Neurological condition was observed by analyzing the ultrastructure of hippocampal synapses. Neuroinflammation was detected by examining microglial activation and proliferation. Toll-like receptor 4 (TLR4)/nuclear factor kappa-B (NF-κB) signaling and NOD-like receptor thermal protein domain associated protein 3 (NLRP3) inflammasomes in the hippocampus were further analyzed. For the study on the role of gut microbiota, the intestinal microbiota of one group was depleted by administering broad-spectrum antibiotic cocktail. Some of the mice in each group were killed at 2 weeks to analyze whether the gut microbiota is altered prior to behavioral changes and to confirm the microbiome-gut-brain axis.

2. Materials And Methods

2.1 Animals and grouping

Sixty-six male C57BL/6J mice aged 3 months were purchased from Shanghai Jihui Laboratory Animal Care Company (Shanghai, China) and housed in a standard specific pathogen-free animal laboratory (temperature 20-26 °C; relative humidity 40-60%; 12 h light–dark cycle) with access to food and liquid ad

libitum. All procedures were performed in accordance with the Guidelines in the Care and Use of Animals and with the approval of the Soochow University Animal Welfare Committee (No. 202009A661). After 1 week of acclimation, the mice were randomly divided into four groups: the CON (n=18), WD (n=18), Lf (n=18), and f+AB (n=12). The mice in the CON group were fed with a standard diet (AIN93G, kcal%: protein 20.3%, carbohydrate 63.9%, and fat 15.8%) and the other three groups were fed with WD (D18061501, kcal%: protein 17%, carbohydrate 43%, and fat 40%). Both diets were purchased from Dyets Inc., (Wuxi, Jiangsu, China) (Table A.1). The mice in the Lf group were intragastrically administered with Lf at 500 mg/kg body weight for five times a week. Native bovine Lf (92.5% purity) was obtained from Hilmar Cheese Company (CA, USA). Lf was prepared as a 65 mg/mL solution in distilled water, and orally administered to mice (i.e., 25–30 g) as an approximately 0.2 ml solution. The mice in the Lf+AB group were administered with Lf and drank solution with antibiotics (ampicillin 1 g/L, vancomycin 0.25 g/L, neomycin 1 g/L,and metronidazole 1 g/L). Drinking water was changed every 2 days. Body weight, diet, and water amounts were recorded weekly. A short-term experiment was performed in the CON, WD, and Lf groups (each group n=6) at 2 weeks. After the cognitive behavior tests, the mice were euthanized and their cecal contents were collected for gut microbiota analyses. The remaining mice in the four groups (each group n=12) were maintained under the same conditions, and the experiments were ended at 16 weeks. The experimental design and animal groups are shown in Fig. A.1.

2.2 Behavioral tests

Nesting behavior test, novel object recognition (NOR) test, and Morris water maze (MWM) test were used to examine recognition memory and spontaneous rodent behaviors. The results were recorded by a video tracking system (SuperMaze software, Shanghai Xinruan Information Technology Co., Ltd., China). In reference to previous studies [17-19], the tests were briefly described as follows.

Nesting behavior test: Approximately 1 h before the dark phase, the mice were transferred to individual testing cages with an unscented paper towel of uniform size. The next morning, the nests were assessed on a rating scale from 1 to 5: 1) paper towels intact; 2) paper towels remain largely intact (>90% complete); 3) paper towels are mostly chopped but no recognizable nest position; 4) a flat nest can be seen and the paper towels are arranged in a certain direction; and 5) the nest is constructed higher than the mouse, and the circumference can completely surround the mouse.

NOR test: The mice were habituated to the testing arena with two identical objects for 10 min for 2 consecutive days. At day 3, the mice were permitted to explore the arena for 10 min for the familiarization phase and then returned to their home cages. After 30 min, one of the objects was replaced with a novel object of similar size and the mice were placed in the testing arena. Short-term object memory was assessed by object exploration defined as an animal's nose approaching the object inside a 2 cm radius around the objects.

MWM test: MWM test was routinely performed using a water maze device with 150 cm diameter and 35 cm high circular pool (XR-XM101, Shanghai Xinruan Information Technology Co. Ltd., Shanghai, China). The mice were individually housed for 1 day and then acquisitively trained over 5 consecutive days with

four trials per day. At day 6, the platform was removed and the mice were returned to the device. Latency to the platform, amount of time spent in the target quadrant, and number of platform crossings were recorded to indicate the degree of memory consolidation.

2.3 Biochemical analyses

At the end of experiment, the mice were deprived of food for 12 hours and sacrificed. Serum was separated by centrifugation (3000 g, at 4 °C for 15 minutes) and stored at −80 °C. Serum total cholesterol (TC), triglyceride (TG), low-density lipoprotein cholesterol (LDL-C), and high-density lipoprotein cholesterol (HDL-C) were detected using commercial kits (Applygen Technologies Inc., Beijing, China). Serum TNF-α and IL-6 were analyzed by ELISA kits (MultiSciences (Lianke) Biotech Co., Ltd., Hangzhou, China).

2.4 Hematoxylin-eosin (HE) staining and immunofluorescence double labeling

The mice from the CON, WD, and Lf groups were perfused via the tips of the heart with phosphate-buffered saline (PBS, pH 7.2) and 4% paraformaldehyde. The mouse brains were then maintained in 4% paraformaldehyde for 48 hours and embedded into paraffin block. The paraffin-embedded brains were sagittally cut into 4 μm-thick slice. For histopathological examination, the sections including cortex and hippocampus (cornuammonis (CA) and and dentate gyrus (DG)) were assessed by routine HE staining. For immunofluorescence double labeling, the sections were blocked by bovine serum albumin and then incubated with primary antibody mixture including mouse anti-BrdU (1:500, Wuhan Servicebio Technology Co., Ltd., Wuhan, China) and rabbit anti-Ibα1 (1:500, Servicebio) overnight at 4 °C. After incubation with the secondary antibodies for 1 h at room temperature in the darkness, DAPI (Invitrogen, CA, USA) was applied for counterstaining and images were taken using Pannoramic Midi (3D Histech Ltd., Budapest, Hungary).

2.5 Analysis of the synapse ultrastructure in the hippocampus

After undergoing transcardial perfusion with saline, the brain tissues were taken out and a 1 mm^3 tissue block was cut from the hippocampus. After being dehydrated in ascending graded ethanol series and embedded in epoxy resin, the block was fixed in 2% paraformaldehyde-2.5% glutaraldehyde mixture for 24 h and treated post-fixation with 1% osmium tetroxide (OsO_4) for 2 h. Sections (70 nm) were cut and stained with 4% uranyl acetate and 0.5% lead citrate. Images were observed under a JEM-1230 transmission electron microscope (TEM) equipped with a side inserted BioScan camera (Veleta, EMSIS GmbH, Germany). Synaptic morphometrics (postsynaptic density, synaptic clefts width, and the curvature of the synaptic interface) were analyzed by the previously described methods (Pan et al., 2021) using Image J software.

2.6 Measurements of colon length and colonic mucus layer thickness

The distal colon was removed quickly, and its length was measured using a high-precision electronic digital caliper (Deli, dl-150, Ningbo, Zhejiang). The colon was cleaned and a part of colon tissues was

stored at −80 °C for further use. The remaining descending colons were fixed in Carnoy's solution. After being washed in anhydrous methanol, the tissues were placed in cassettes and stored in anhydrous methanol. For the detection of colonic mucus layer thickness, the tissues were embedded in paraffin and cut into 5 μm-thick slice. After mounting on glass slides with Alcian blue staining, the thickness of colonic mucus layer was observed under an eclipse microscope (Nikon, Tokyo, Japan).

2.7 Quantitative real-time polymerase chain reaction (qRT-PCR) analysis

Total mRNA was extracted from the tissues using the RNA quick purification kit (Yeasen Biotechnology, Shanghai, China), and cDNA was synthesized using Hifair® 1st Strand cDNA Synthesis SuperMix (Yeasen Biotechnology, Shanghai, China) and GeneAmp PCR system 9700 (Applied Biosystems) following the manufacturer's instructions. qRT-PCR was performed using Hieff® qPCR SYBR Green Master Mix (Yeasen Biotechnology, Shanghai, China) and QuantStudio 6 Flex Real-Time PCR System (Thermo, USA). Relative mRNA expression level was determined using the 2-ΔΔCt method with GAPDH as the internal reference control [20]. Table A.2 shows the gene-specific mouse primers.

2.8 Western blot analysis

The tissues were homogenized in ice-cold RIPA lysis buffer (Beyotime, Shanghai, China) and supplemented with complete EDTA-free protease inhibitor cocktail and PhosSTOP Phosphatase Inhibitor. The protein samples were mixed with 5× dual color protein loading buffer (Fudebio, Hangzhou, China) and boiled at 98 °C for 10 min. Equal amounts of protein (30 μg/lane) were loaded on a SDS-PAGE gel at a constant voltage and then transferred to a polyvinylidene difluoride membrane (Millipore, MA, USA). After being blocked and incubated with the primary and secondary antibodies, the bands were visualized using a chemiluminescence image analysis system (Tanon, Shanghai, China) with FDbioFemto ECL (Fudebio, Hangzhou, China). The band intensities were quantified using Gel-Pro Analyzer software (Media Cybernetics, Maryland, USA). The primary antibodies were included the following: synaptosomal associated proteins 25 (SNAP-25 ; Abcam, ab109105), postsynaptic density proteins 95 (PSD-95; CST, 3450), Ibα1 (Abcam, ab178846), TNF-α (Abcam, ab215188), IL-6 (Abcam, ab233706), NLRP3 (Abcam, ab263899), IL-18(Abcam, ab243091), IL-1β (Abcam, ab254360), caspase-1 (Abcam, ab207802), TLR4 (Abcam, ab22048), myeloid differentiation factor 88 (MyD88; Abcam, ab133739), aNF-κB p65 (Abcam, ab32536), GAPDH (ABclonal, AC033), ZO-1 (ABclonal, A11417), occludin (ABclonal, A12621) and β-actin (ABclonal, AC026).

2.9 16S rRNA Gene Sequencing and Analysis

DNA was extracted by a PowerMax extraction kit (MoBio Laboratories, CA, USA) following the product introduction. The V3-V4 region of the bacteria's 16S rRNA gene was amplified by a thermocycler PCR system. PCR products were purified using AMPure XP Beads (Beckman Coulter, IN, USA) and quantified using PicoGreen dsDNA Assay Kit (Invitrogen); Finally the sequencing was conducted using 2×150 bp pair-end configuration on Illumina HiSeq4000 platform. The 16S rRNA data were analyzed using Quantitative Insights into Microbial Ecology (QIIME) and R package (v3.2.0). Quality filtering was

performed to obtain the effective sequence, and the effective sequence clustering with 97% confidence threshold was grouped into operation taxonomic units (OTUs) by Vsearchv2.4.4. Representative sequences of OTUs were selected and annotated based on SILVA128. The community composition of each sample and the abundance of OTUs were counted at the levels of kingdom, phylum, class, order, family, genus, and species. Alpha diversity index (including Chao1, abundance-based coverage estimator (ACE), Shannon and Simpson indexes) was calculated with QIIME software to compare OTUs abundance, evenness, and difference between groups. Linear discriminant analysis effect size (LefSe) was used to select the biomarkers for comparison among the groups.

2.10 Statistical analysis

Data were analyzed using the statistical package SPSS (Version 20, Chicago, USA). Differences among the intervention groups were determined using one-way analysis of variance (ANOVA) followed by least significant difference (LSD, if homogeneity of variance was satisfied) or Tamhane's T2 (if homogeneity of variance was not satisfied) for multiple comparisons. A p value of < 0.05 was considered to be statistically significant. For 16S rRNA gene sequencing analysis, all reads were deposited and grouped into OTU at a sequence identity of 97%. The taxonomic affiliation of the OTUs was determined with quantitative insights into microbial ecology (QIIME, version 1.8.0) against the Greengenes database version 13.8.

3. Results

3.1 Lf intervention decreased body weight and improved lipid profiles

During the experimental period, the mice fed with WD had heavier body weights than those fed with standard diet. However, the body weight was significantly lower in the Lf group than in the WD group (Figs. 1A and B). WD feeding resulted in significant accumulation of white adipose tissues. A significant decrease in the weight of subcutaneous, perirenal and epididymal fats was observed in the Lf group (Fig. 1C). Although the mice in the WD group had less food intake, there were no significant difference in energy intake among the three groups (Fig. 1D). WD feeding caused dyslipidemia due to increased serum TC, TG, and LDL and decreased serum HDL in the WD group. This phenomenon was reversed in the Lf group (Figs. 1E-H).

3.2 Lf intervention ameliorated cognitive impairment

Nesting behavior was impaired by WD improved by Lf intervention (Fig. 2A) as quantitatively confirmed by the nesting score (Fig. 2B). In the NOR test, the mice in the WD group had significantly decreased number of head explorations and exploration time with novel object. These two indexes were restored by Lf intervention, suggesting the improvement of novel object recognition memory (Figs. 2C-E). The total exploration time of objects was comparable among the three groups (Fig. 2F). In the MWM test, the mice in the WD group spent more time and distance to find the platform from the third day. However, the time and distance significantly reduced in the Lf group compared with the WD group (Figs. 2G-

I). Meanwhile, the decreased time spent in the target quadrant and numbers crossing platform in the WD group was significantly restored in the Lf group (Figs. 2J-M). Thus, Lf ameliorated the WD-induced impairment of cognitive function.

3.3 Lf intervention improved the hippocampal neurons and synapses

The hippocampus and cortex are main regions implicated in cognitive processing, learning, and memory. HE staining showed that the mice in the CON group had normal morphology of neurons in the hippocampus region. Swollen neurons with a loose structure, increased nuclear pyknosis, and neuronal damages were observed in the WD group; these neuronal pathological changes were partially ameliorated in the Lf group (Fig. 3A). TEM analysis showed that WD feeding reduced the length, width, and curvature of the PSD in the hippocampus region (Fig. 3B). Quantitatively, their length and curvature were significantly higher in the Lf group than in the WD group (Figs. 3C-E). Meanwhile, the decreased protein expression levels of PSD-95 and SNAP-25 in the WD group were significantly upregulated in the Lf group (Figs. 3F-H). Thus, Lf improved the WD-induced damage of hippocampal neurons and synapses.

3.4 Lf intervention suppressed microglia activation and inflammation in the brain

The hippocampus and cortex are particularly vulnerable to inflammation [21, 22]. With Ibα1 acting as the marker of microglial activation in the brain [23], immunofluorescence analysis showed that WD feeding increased the number of activated microglia in the hippocampal regions. However, the number of activated microglia with $Ibα1^+$ was significantly lower in the Lf group than in the WD group (Figs. 4A and B). BrdU is incorporated in the S-phase cells in the cell cycle and commonly used to detect cell proliferation [24]. Double staining further showed significantly more $BrdU^+$ $Ibα1^+$ positive cells in the WD group than in the CON group, and these positive cells were inhibited in the Lf group (Figs. 4A and C). Meanwhile, WD feeding significantly upregulated the protein expression levels of TNF-α and IL-6 in the cortex and hippocampus, which were significantly inhibited by Lf intervention (Figs. 4F and G). Similarly, compared with those in the CON group, the serum levels of TNF-α and IL-6 significantly increased in the WD group, but were significantly lower in the Lf group than in the WD group (Figs. 4H and I). Thus, Lf prevented the WD-induced microglia activation and neuroinflammation.

3.5 Lf intervention inhibited the activation of NF-κB/NLRP3 inflammasomes in the hippocampus

NF-κB/NLRP3 inflammasomes signaling pathways in the hippocampus were detected by PCR and Western blot. The results showed that the mRNA and protein expression of NF-κB p65 and MyD88 levels were upregulated in the WD group. NF-κB can be activated by TLR4, which was also upregulated by WD. By contrast, Lf intervention downregulated the mRNA and protein expression of TLR4, MyD88, and NF-κB p65 (Figs. 5A-C). Stimulation of the NF-κB signal transduction pathway is an early event for NLRP3 inflammasome activation [25]. The results showed that the mRNA and protein expression of NLRP3, caspase-1, IL-18, and IL-1β were significantly higher in the WD group than in the CON group. Nevertheless, Lf significantly downregulated the expression of these four proteins, and the mRNA of IL-18 and IL-1,

compared with those in the WD group (Figs. 5D-F).Therefore, Lf inhibited the WD-induced activation of NF-κB/NLRP3 inflammasome signaling pathway in the hippocampus.

3.6 Lf intervention maintained colonic integrity and alleviated inflammation

Colonic physiological function is dependent on its length. At autopsy, the colon of the mice in the WD group was shortened by 10.12%. It was restored by Lf intervention almost to the same length in the CON group (Figs. 6A and B). Alcian blue staining showed that the mucosal thickness in the colon was decreased in the WD group compared with that in the CON group, and was increased by Lf intervention (Fig. 6C). In terms of the integrity of gut barrier, the expression of tight junction proteins occludin and ZO-1 was significantly downregulated in the WD group, but upregulated in the Lf group. Significant difference in ZO-1 protein was observed in the Lf group compared with that in the WD group (Figs. 6D and E). Given that shortened colon length and damaged colonic integrity are associated with inflammation, further analysis revealed that Lf intervention significantly inhibited the WD-induced upregulation of protein expression of TNF-α, IL-6, and IL-1β in the colon tissues (Figs. 6F and G). These results indicated that Lf maintained colonic function, which provides the basis for gut microbiota.

3.7 Lf intervention improved gut microbiota alteration

The effects of Lf on the community structure of the gut microbiota were investigated by 16S rRNA gene-based profiling of fecal microbiota. The α diversity of the gut microbiota was assessed by Chao 1, Shannon indices, and ACE, all of which reflect species richness. Compared with the CON group, the WD group presented a decrease in α diversity in the gut microbiota. Meanwhile, Lf intervention significantly increased the mean community diversity indices (Chao1 and Shannon) compared with those in the WD group (Figs. 7A–C). Principal coordinate analysis (PCoA) of the colonic microbiota community revealed a separated microbial cluster of three groups, and unweighted unifrac test indicated that the abundance of the gut microbiota accounted for 42.33% and 11.08% difference of the total variations. (Figs. 7D and E). Figs. A.2 show the differences among the three groups at the phylum, class, and family levels, respectively. The dominant bacteria are Firmicutes, Bacteroidetes, Deferribacteres, and Proteobacteria for the phylum level; Clostridia, Bacteroidia, Deferribacteres, and Deltaproteobacteria for the class level; and Ruminococcaceae, S24-7, Lachnospiraceae, and Desulfovibrionaceae for the family level. WD feeding significantly decreased the relative abundance of Bacteroidetes and Proteobacteria and increased Firmicutes compared with those in the CON group. However, Lf restored the abundance of Bacteroidetes and Proteobacteria to thelevel in the CON group. WD feeding increased ratio of Firmicutes/Bacteroidetes (F/B), which was reversed by Lf intervention, although no significant difference was observed among the three groups (Fig. 7F). LEfSe analysis indicated that bacteria belonging to the Firmicutes phylum, Tenericutes class, Clostridiales order, and *Roseburia* genus were differentially enriched in the gut bacterial communities (Linear discriminant analysis score > 3) of the CON and WD groups (Figs. 7G and H). Lf intervention regulated the WD-induced shift in microbiome composition by increasing the relative abundances of Bacteroidetes phylum and Roseburia genus (Figs. 7I and J). Further analysis was conducted on the relationship between the gut microbiota and behavior test results using Spearman's

correlation. Cognitive function was found to be positively correlated with phylum Bacteroidetes and Verrucomicrobia, and genus *Odoribacter*, but negatively correlated with phylum Proteobacteria and Actinobacteria, and genus *AF 12* (Fig. A.2).

3.8 Antibiotics eliminated the benefit of long-term Lf intervention in cognitive impairment

A cocktail of oral antibiotics led to a 20-fold reduction in fecal bacterial load (Fig. 8A). Compared with those in the Lf group, the mice in the Lf+AB group gained more body weight and had heavier subcutaneous fat at autopsy (Figs. 8B and C). Meanwhile, the mice in the Lf+AB group had less nesting score (Fig. 8D). No significant differences in other indexes for behavioral tests were found between the two groups (Figs. 8E-H). Thus, the cognitive improvement effect of Lf partly disappeared when the gut microbiota was removed.

3.9 Short-term Lf intervention prevented WD-induced gut microbiota alteration prior to the behavioral cognitive changes

Lf intervention for 2 weeks did not affect cognitive function in the WD-fed mice based on the behavior tests (Figs. 9A-E). However, WD feeding decreased the α diversity in the gut microbiota, which was partly restored by Lf intervention (Figs. 9F-H). PCoA analysis showed that the gut microbial profile in the Lf group was clustered clearly separately from that in the WD group (Fig. 9H). Furthermore, the increased proportion of Firmicutes and decreased proportion of Bacteroidetes in the WD group were restored by Lf intervention (Fig. 9J). Thus, the short-term Lf intervention regulated the gut microbial profile prior to the changes of cognitive function.

4. Discussion

Accumulating evidence indicates that WD high in fat and sugar impairs some aspects of cognition [26]. Imbalance of the microbiome-gut-brain axis plays an important role in cognitive function [2, 5]. Lf prevents memory impairment and influences gut microbiota [15, 16, 27], but its association with gut microbial dysbiosis in cognitive impairment is less well-established. In this study, WD feeding for 16 weeks resulted in cognitive impairment and gut microbial dysbiosis in mice. Importantly, the space in the microbiome-gut-brain axis was resolved. The results showed that antibiotics eliminated the effects of long-term Lf intervention on cognitive impairment, suggesting that the gut microbiota participated in Lf action. In addition, short-term Lf intervention prevented WD-induced gut microbiota alteration without inducing behavioral changes, thus supporting the timing sequence of gut microbiota to brain. Thus, Lf ameliorated the cognitive impairment by improving the gut-microbiome-gut-brain axis.

In the present study, nesting behavior test, NOR test, and MWM test were performed to explore hippocampus-dependent recognition memory and ability to perform activities of daily living [17-19]. The findings showed that Lf inhibited the WD-induced detriment of working learning and memory ability. Aging may decline the spatial learning ability and impaired spatial memory retrieval ability. Using MWM test, Zheng et al. found that Lf gavage for 3 months partially restored spatial cognition in 16-

month-old C57/BL6J mice [28]. Abdelhamid et al. used the preference index to measure cognitive function in NOR tests and found that hydrolyzed Lf feeding for 3 months induced a preference for novel object in APP-Tg mice [15]. Xu et al. also found that peritoneally Lf injection for 1 week substantially ameliorated PD-like motor dysfunction in mouse model [29]. Thus, Lf is beneficial for the impaired cognitive function in various animal models with neurodegenerative diseases. The findings were further demonstrated in the hippocampus, which is involved in cognitive processing, learning, and memory.

The dysregulation of synaptic formation and plasticity in the hippocampus has been implicated in cognitive impairment and AD [30]. As expected, WD disrupted the hippocampal ultrastructural synaptic architecture and Lf effectively reversed the morphological damage of postsynaptic density. PSD-95 is a member of the PSD family and plays an important role in synaptic integration and neural function recovery [31]. SNAP-25 is a member of the receptor family of soluble N-ethyl maleimide sensitive factor attachment proteins and regulates the extracellular secretion of synaptic vesicles [32]. This study demonstrated that Lf significantly upregulated the expression of synaptic functional proteins SNAP-25 and PSD-95 in the hippocampus. Together with the results on related protein expression, this finding supported that Lf retard the WD-induced impairment of cognitive function.

Microglia are the resident immune cells of the brain that become activated in response to infectious insult and other injuries. Excessive microglial activation can damage the surrounding healthy neural tissues. In turn, and the factors secreted by the dead or dying neurons exacerbate the chronic activation of microglia, causing progressive loss of neurons, and then cognitive impairment [33]. Immunofluorescence analysis showed that Lf inhibited the WD-induced microglial activation in the hippocampal regions. Activated microglia produce a wide spectrum of proinflammatory cytokines, which ultimately induce neuronal damage [34]. Similarly, Lf intervention downregulated the expression of TNF-α and IL-6 in the cortex and hippocampus. On the other hand, circulation cytokines can reach the brain via the cytokine transporters expressed by the endothelial cells of the blood-brain barrier and subsequently modulate the cytokine production of microglia [35]. Zheng et al. found that Lf reduced the hippocampal and serum levels of IL-1β, IL-6, and TNF-α in aged mice [28]. In the present work, the cross-talk of peripheral and central inflammation was observed because Lf simultaneously alleviated the serum levels of TNF-α and IL-6.

As the first-line host defense against invading pathogens on the surface of microglia, TLR4 activates multiple downstream signaling pathways, such as NF-κB signaling pathways [36]. After binding with Aβ, TLR4 can activate NF-κB complex and downstream events that participate in the transcriptional expression of NLRP3 and pro-IL-β [37]. In normal inflammatory cells, activated TLR4 can bind directly to intracellular protein myeloid differentiation factor MyD88. MyD88 upregulation can further increase the expression of inflammatory cytokines such as TNF-α and IL-1β [38]. On the other hand, NF-κB mediates the formation of NLRP3 inflammasome, which recruits and polymerizes ASC, leading to caspase-1 activation. An activated caspase-1 promotes the maturity and release of pro-inflammatory cytokines[39]. As a result, numerous neuroinflammation processes further exacerbate the pathological processes that cause cognitive impairment [40]. The inflammatory signaling pathway NF-κB/NLRP3/caspase-1 is activated in a variety of cells [39, 41]. In this study, NF-κB/NLRP3 inflammasome

activation was found to be involved in neuroinflammation caused by WD feeding. Lf intervention inhibited the WD-induced upregulation of NF-κB/NLRP3/caspase-1/IL-1β/IL-18 axis. The benefit of Lf on NF-κB/NLRP3 inflammasome was previously observed on other cells or organ injury. Nemati et al. demonstrated that Lf downregulated TLR4, MyD88, IL-6, and TNF-α expression in lipopolysaccharide-activated murine RAW264.7 cells [42]. Madkour et al. found that Lf administration significantly ameliorated glycerol-induced rhabdomyolysis and acute kidney injury by decreasing renal IL-1β, NLRP3 and NF-κB [43]. As far as we know, this work is the first to demonstrate the anti-inflammation effects of Lf may be related to its inhibition of NF-κB/NLRP3 inflammasome activation in the hippocampus.

Impaired gut permeability allows for the influx of adverse substances and disrupts gut bacterial ecosystem [44]. Gut microbiota has potential effects on gut permeability [45]. Obese-type microbiota transplantation disrupts intestinal barrier function and induces cognitive decline in mice [9]. In this study, WD diet intake dramatically increased intestinal inflammation and diminished intestinal barrier integrity, which was consistent with previous studies [26]. Lf intervention increased colon length, upregulated colonic tight-junction protein occludin, and lowered the colonic inflammation. Similarly, Hu et al. found that Lf treatment restored the deoxynivalenol- induced damage of mouse intestinal integrity by enhancing the occludin expression and reducing the production of proinflammatory cytokines [46].

The gut microbiota exerts its action at least in part by modulating neuroinflammation. Microglia are involved in the development of neuroinflammation and are mediated by the gut microbiota [35]. An altered gut microbiota was found to be positively correlated with microgliosis and increased cerebral NLRP3 inflammasome and IL-1β in a mouse model of AD [47]. Transplantation of the gut microbiota of AD patients induced the activation of NLRP3 inflammasome and caused the release of inflammatory factors in the intestinal tract of mice [8]. By contrast, the transplantation of healthy fecal microbiota protected the PD mice by suppressing neuroinflammation and inhibiting TLR4/TNF-α signaling pathway [48]. In the present study, Lf restored the WD-induced decrease in the α diversity of the gut microbiota, which was consistent with the findings of other studies using suckling piglets [49] and APP/PS1 mice [16]. Thus, the observed benefits of Lf on cognitive impairment, neuroinflammation, and NF-κB/NLRP3 inflammasomes in the hippocampus are possibly linked to the gut microbiota.

Bacteroidetes are beneficial for gut barrier [50] and Bacteroidetes is associated with AD [51]. In a cross-section study, a low Bacteroidetes abundance was found in the gut microbiota of dementia patients [52]. In the current work, Lf restored the WD-induced decrease in Bacteroidetes and improved epithelial damage and memory impairment. Correlation analysis further indicated that cognitive function was positively correlated with Bacteroidetes. Therefore, Lf regulated Bacteroidetes in the microbiome-gut-brain axis to alleviate cognitive impairment. Firmicutes and Bacteroidetes are two major phyla of bacteria in the intestine, and the F/B ratio is significantly increased in obese mice [53]. In humans, the F/B ratio increases several folds with aging, a major risk of neurodegenerative diseases [54]. In the present study, Lf intervention tended to decrease F/B ratio, which was consistent with other study using high-fat diet mice treated with Lf[55]. *Roseburia* genus are associated with obesity and neurodegenerative diseases [56-58]. A systematic search found that *Roseburia* is the lean-associated genus in the Eastern

population [59]. Hu et al. found that suckling piglets drank Lf containing solution had a high *Roseburia* abundance [49]. In the present work, Lf intervention increased the abundance of *Roseburia*, which is probably linked to the improvement of cognitive impairment.

Overall, our findings demonstrated the beneficial effects of Lf intervention on the cognitive impairment of WD-induced obese mice by alleviating synaptic damages and inhibiting microglial activation. The underlying mechanism involved the decreased neuroinflammation by inhibiting the activation of NF-κB/NLRP3 inflammasomes and ameliorating the shift in gut microbiota composition through the microbiome-gut-brain axis.

Declarations

Data availability statement

The data that support the findings of this study are available from the corresponding authors upon reasonable request.

Ethics approval and consent to participate

All procedures were performed in accordance with the Guidelines in the Care and Use of Animals and with the approval of the Soochow University Animal Welfare Committee (No. 202009A661).

Consent for publication

Not applicable.

Competing interests

The authors declare that they have no known competing financial interests or personal relationships that could have appeared to influence the work reported in this paper.

Funding

This work was supported the National Natural Science Foundation of China (no. 82173502, and 81973024), Key LaboratoryOpen Project for State Key Laboratory of Radiation Medicine and Protection (GZK1202001), and Priority Academic Program Development of Jiangsu Higher Education Institutions (PAPD).

Authors' contributions

QLQ, XJY, and WPH contributed to the conception and design of the study. HQ, WJX, LDM, GYX and WQY performed the experiments. HQ, WJX and LDM contributed to the analysis of data. HQ contributed to preparing the tables and figures. HQ prepared the manuscript. HQ, WJX, LDM, QLQ, XJY, and WPH helped in the editing of the manuscript. All authors read and approved the final manuscript.

References

1. Fan JG, Kim SU, Wong VW: New trends on obesity and NAFLD in Asia. *J Hepatol* 2017, 67:862-873.
2. Leigh SJ, Morris MJ: Diet, inflammation and the gut microbiome: Mechanisms for obesity-associated cognitive impairment. *Biochim Biophys Acta Mol Basis Dis* 2020, 1866:165767.
3. Farruggia MC, Small DM: Effects of adiposity and metabolic dysfunction on cognition: A review. *Physiol Behav* 2019, 208:112578.
4. Kwon HS, Koh SH: Neuroinflammation in neurodegenerative disorders: the roles of microglia and astrocytes. *Transl Neurodegener* 2020, 9:42.
5. Buford TW: (Dis)Trust your gut: the gut microbiome in age-related inflammation, health, and disease. *Microbiome* 2017, 5:80.
6. Diaz Heijtz R, Wang S, Anuar F, Qian Y, Bjorkholm B, Samuelsson A, Hibberd ML, Forssberg H, Pettersson S: Normal gut microbiota modulates brain development and behavior. *Proc Natl Acad Sci U S A* 2011, 108:3047-3052.
7. Liu S, Gao J, Zhu M, Liu K, Zhang HL: Gut Microbiota and Dysbiosis in Alzheimer's Disease: Implications for Pathogenesis and Treatment. *Mol Neurobiol* 2020, 57:5026-5043.
8. Shen H, Guan Q, Zhang X, Yuan C, Tan Z, Zhai L, Hao Y, Gu Y, Han C: New mechanism of neuroinflammation in Alzheimer's disease: The activation of NLRP3 inflammasome mediated by gut microbiota. *Prog Neuropsychopharmacol Biol Psychiatry* 2020, 100:109884.
9. Bruce-Keller AJ, Salbaum JM, Luo M, Blanchard Et, Taylor CM, Welsh DA, Berthoud HR: Obese-type gut microbiota induce neurobehavioral changes in the absence of obesity. *Biol Psychiatry* 2015, 77:607-615.
10. Livingston G, Sommerlad A, Orgeta V, Costafreda SG, Huntley J, Ames D, Ballard C, Banerjee S, Burns A, Cohen-Mansfield J, et al: Dementia prevention, intervention, and care. *The Lancet* 2017, 390:2673-2734.
11. Brimelow RE, West NP, Williams LT, Cripps AW, Cox AJ: A role for whey-derived lactoferrin and immunoglobulins in the attenuation of obesity-related inflammation and disease. *Crit Rev Food Sci Nutr* 2017, 57:1593-1602.
12. Reseco L, Atienza M, Fernandez-Alvarez M, Carro E, Cantero JL: Salivary lactoferrin is associated with cortical amyloid-beta load, cortical integrity, and memory in aging. *Alzheimers Res Ther* 2021, 13:150.
13. Mohamed WA, Salama RM, Schaalan MF: A pilot study on the effect of lactoferrin on Alzheimer's disease pathological sequelae: Impact of the p-Akt/PTEN pathway. *Biomed Pharmacother* 2019, 111:714-723.
14. Guo C, Yang ZH, Zhang S, Chai R, Xue H, Zhang YH, Li JY, Wang ZY: Intranasal Lactoferrin Enhances alpha-Secretase-Dependent Amyloid Precursor Protein Processing via the ERK1/2-CREB and HIF-1alpha Pathways in an Alzheimer's Disease Mouse Model. *Neuropsychopharmacology* 2017, 42:2504-2515.

15. Abdelhamid M, Jung CG, Zhou C, Abdullah M, Nakano M, Wakabayashi H, Abe F, Michikawa M: Dietary Lactoferrin Supplementation Prevents Memory Impairment and Reduces Amyloid-beta Generation in J20 Mice. *J Alzheimers Dis* 2020, 74:245-259.
16. Zhou HH, Wang G, Luo L, Ding W, Xu JY, Yu Z, Qin LQ, Wan Z: Dietary lactoferrin has differential effects on gut microbiota in young versus middle-aged APPswe/PS1dE9 transgenic mice but no effects on cognitive function. *Food Nutr Res* 2021, 65.
17. Bevins RA, Besheer J: Object recognition in rats and mice: a one-trial non-matching-to-sample learning task to study 'recognition memory'. *Nat Protoc* 2006, 1:1306-1311.
18. Deacon RM: Assessing nest building in mice. *Nat Protoc* 2006, 1:1117-1119.
19. Vorhees CV, Williams MT: Morris water maze: procedures for assessing spatial and related forms of learning and memory. *Nat Protoc* 2006, 1:848-858.
20. Livak KJ, Schmittgen TD: Analysis of relative gene expression data using real-time quantitative PCR and the 2(-Delta Delta C(T)) Method. *Methods* 2001, 25:402-408.
21. Dinel AL, Andre C, Aubert A, Ferreira G, Laye S, Castanon N: Lipopolysaccharide-induced brain activation of the indoleamine 2,3-dioxygenase and depressive-like behavior are impaired in a mouse model of metabolic syndrome. *Psychoneuroendocrinology* 2014, 40:48-59.
22. Jeon BT, Jeong EA, Shin HJ, Lee Y, Lee DH, Kim HJ, Kang SS, Cho GJ, Choi WS, Roh GS: Resveratrol attenuates obesity-associated peripheral and central inflammation and improves memory deficit in mice fed a high-fat diet. *Diabetes* 2012, 61:1444-1454.
23. Lituma PJ, Woo E, O'Hara BF, Castillo PE, Sibinga NES, Nandi S: Altered synaptic connectivity and brain function in mice lacking microglial adapter protein Iba1. *Proc Natl Acad Sci U S A* 2021, 118.
24. Cheng X, Yeung PKK, Zhong K, Zilundu PLM, Zhou L, Chung SK: Astrocytic endothelin-1 overexpression promotes neural progenitor cells proliferation and differentiation into astrocytes via the Jak2/Stat3 pathway after stroke. *J Neuroinflammation* 2019, 16:227.
25. Bauernfeind FG, Horvath G, Stutz A, Alnemri ES, MacDonald K, Speert D, Fernandes-Alnemri T, Wu J, Monks BG, Fitzgerald KA, et al: Cutting edge: NF-kappaB activating pattern recognition and cytokine receptors license NLRP3 inflammasome activation by regulating NLRP3 expression. *J Immunol* 2009, 183:787-791.
26. Kendig MD, Leigh SJ, Morris MJ: Unravelling the impacts of western-style diets on brain, gut microbiota and cognition. *Neurosci Biobehav Rev* 2021, 128:233-243.
27. Tsatsanis A, McCorkindale AN, Wong BX, Patrick E, Ryan TM, Evans RW, Bush AI, Sutherland GT, Sivaprasadarao A, Guennewig B, Duce JA: The acute phase protein lactoferrin is a key feature of Alzheimer's disease and predictor of Abeta burden through induction of APP amyloidogenic processing. *Mol Psychiatry* 2021, 26:5516-5531.
28. Zheng JP, Xie YZ, Li F, Zhou Y, Qi LQ, Liu LB, Chen Z: Lactoferrin improves cognitive function and attenuates brain senescence in aged mice. *JOURNAL OF FUNCTIONAL FOODS* 2020, 65.
29. Xu SF, Zhang YH, Wang S, Pang ZQ, Fan YG, Li JY, Wang ZY, Guo C: Lactoferrin ameliorates dopaminergic neurodegeneration and motor deficits in MPTP-treated mice. *Redox Biol* 2019,

21:101090.

30. Lamont MG, Weber JT: The role of calcium in synaptic plasticity and motor learning in the cerebellar cortex. *Neurosci Biobehav Rev* 2012, 36:1153-1162.
31. Ugalde-Trivino L, Diaz-Guerra M: PSD-95: An Effective Target for Stroke Therapy Using Neuroprotective Peptides. *Int J Mol Sci* 2021, 22.
32. Shaaban A, Dhara M, Frisch W, Harb A, Shaib AH, Becherer U, Bruns D, Mohrmann R: The SNAP-25 linker supports fusion intermediates by local lipid interactions. *Elife* 2019, 8.
33. Bao LH, Zhang YN, Zhang JN, Gu L, Yang HM, Huang YY, Xia N, Zhang H: Urate inhibits microglia activation to protect neurons in an LPS-induced model of Parkinson's disease. *J Neuroinflammation* 2018, 15:131.
34. Banati RB: Visualising microglial activation in vivo. *Glia* 2002, 40:206-217.
35. Bairamian D, Sha S, Rolhion N, Sokol H, Dorothee G, Lemere CA, Krantic S: Microbiota in neuroinflammation and synaptic dysfunction: a focus on Alzheimer's disease. *Mol Neurodegener* 2022, 17:19.
36. Lu YC, Yeh WC, Ohashi PS: LPS/TLR4 signal transduction pathway. *Cytokine* 2008, 42:145-151.
37. Zhou X, Yuan L, Zhao X, Hou C, Ma W, Yu H, Xiao R: Genistein antagonizes inflammatory damage induced by beta-amyloid peptide in microglia through TLR4 and NF-kappaB. *Nutrition* 2014, 30:90-95.
38. Zhao M, Zhou A, Xu L, Zhang X: The role of TLR4-mediated PTEN/PI3K/AKT/NF-kappaB signaling pathway in neuroinflammation in hippocampal neurons. *Neuroscience* 2014, 269:93-101.
39. Yu S, Ren X, Meng F, Guo X, Tao J, Zhang W, Liu Z, Fu R, Li L: TIM3/CEACAM1 pathway involves in myeloid-derived suppressor cells induced CD8(+) T cells exhaustion and bone marrow inflammatory microenvironment in myelodysplastic syndrome. *Immunology* 2022.
40. Holmes C: Review: systemic inflammation and Alzheimer's disease. *Neuropathol Appl Neurobiol* 2013, 39:51-68.
41. Hua F, Li JY, Zhang M, Zhou P, Wang L, Ling TJ, Bao GH: Kaempferol-3-O-rutinoside exerts cardioprotective effects through NF-kappaB/NLRP3/Caspase-1 pathway in ventricular remodeling after acute myocardial infarction. *J Food Biochem* 2022:e14305.
42. Nemati M, Akseh S, Amiri M, Reza Nejabati H, Jodati A, Fathi Maroufi N, Faridvand Y, Nouri M: Lactoferrin suppresses LPS-induced expression of HMGB1, microRNA 155, 146, and TLR4/MyD88/NF-small ka, CyrillicB pathway in RAW264.7 cells. *Immunopharmacol Immunotoxicol* 2021, 43:153-159.
43. Madkour AH, Helal MG, Said E, Salem HA: Dose-dependent renoprotective impact of Lactoferrin against glycerol-induced rhabdomyolysis and acute kidney injury. *Life Sci* 2022, 302:120646.
44. Malesza IJ, Malesza M, Walkowiak J, Mussin N, Walkowiak D, Aringazina R, Bartkowiak-Wieczorek J, Madry E: High-Fat, Western-Style Diet, Systemic Inflammation, and Gut Microbiota: A Narrative Review. *Cells* 2021, 10.

45. Paone P, Cani PD: Mucus barrier, mucins and gut microbiota: the expected slimy partners? *Gut* 2020, 69:2232-2243.
46. Hu P, Zong Q, Zhao Y, Gu H, Liu Y, Gu F, Liu HY, Ahmed AA, Bao W, Cai D: Lactoferrin Attenuates Intestinal Barrier Dysfunction and Inflammation By Modulating the MAPK Pathway and Gut Microbes in Mice. *J Nutr* 2022.
47. Shukla PK, Delotterie DF, Xiao J, Pierre JF, Rao R, McDonald MP, Khan MM: Alterations in the Gut-Microbial-Inflammasome-Brain Axis in a Mouse Model of Alzheimer's Disease. *Cells* 2021, 10.
48. Sun MF, Zhu YL, Zhou ZL, Jia XB, Xu YD, Yang Q, Cui C, Shen YQ: Neuroprotective effects of fecal microbiota transplantation on MPTP-induced Parkinson's disease mice: Gut microbiota, glial reaction and TLR4/TNF-alpha signaling pathway. *Brain Behav Immun* 2018, 70:48-60.
49. Hu P, Zhao F, Wang J, Zhu W: Early-life lactoferrin intervention modulates the colonic microbiota, colonic microbial metabolites and intestinal function in suckling piglets. *Appl Microbiol Biotechnol* 2020, 104:6185-6197.
50. Desai MS, Seekatz AM, Koropatkin NM, Kamada N, Hickey CA, Wolter M, Pudlo NA, Kitamoto S, Terrapon N, Muller A, et al: A Dietary Fiber-Deprived Gut Microbiota Degrades the Colonic Mucus Barrier and Enhances Pathogen Susceptibility. *Cell* 2016, 167:1339-1353 e1321.
51. Doifode T, Giridharan VV, Generoso JS, Bhatti G, Collodel A, Schulz PE, Forlenza OV, Barichello T: The impact of the microbiota-gut-brain axis on Alzheimer's disease pathophysiology. *Pharmacol Res* 2021, 164:105314.
52. Saji N, Niida S, Murotani K, Hisada T, Tsuduki T, Sugimoto T, Kimura A, Toba K, Sakurai T: Analysis of the relationship between the gut microbiome and dementia: a cross-sectional study conducted in Japan. *Sci Rep* 2019, 9:1008.
53. Koliada A, Syzenko G, Moseiko V, Budovska L, Puchkov K, Perederiy V, Gavalko Y, Dorofeyev A, Romanenko M, Tkach S, et al: Association between body mass index and Firmicutes/Bacteroidetes ratio in an adult Ukrainian population. *BMC Microbiol* 2017, 17:120.
54. Ley RE, Turnbaugh PJ, Klein S, Gordon JI: Human gut microbes associated with obesity. *Nature* 2006, 444:1022-1023.
55. Li L, Ma C, Hurilebagen, Yuan H, Hu R, Wang W, Weilisi: Effects of lactoferrin on intestinal flora of metabolic disorder mice. *BMC Microbiol* 2022, 22:181.
56. Karlsson FH, Tremaroli V, Nookaew I, Bergstrom G, Behre CJ, Fagerberg B, Nielsen J, Backhed F: Gut metagenome in European women with normal, impaired and diabetic glucose control. *Nature* 2013, 498:99-103.
57. Keshavarzian A, Green SJ, Engen PA, Voigt RM, Naqib A, Forsyth CB, Mutlu E, Shannon KM: Colonic bacterial composition in Parkinson's disease. *Mov Disord* 2015, 30:1351-1360.
58. Neyrinck AM, Possemiers S, Verstraete W, De Backer F, Cani PD, Delzenne NM: Dietary modulation of clostridial cluster XIVa gut bacteria (Roseburia spp.) by chitin-glucan fiber improves host metabolic alterations induced by high-fat diet in mice. *J Nutr Biochem* 2012, 23:51-59.

59. Xu Z, Jiang W, Huang W, Lin Y, Chan FKL, Ng SC: Gut microbiota in patients with obesity and metabolic disorders - a systematic review. *Genes Nutr* 2022, 17:2.

Figures

Fig. 1

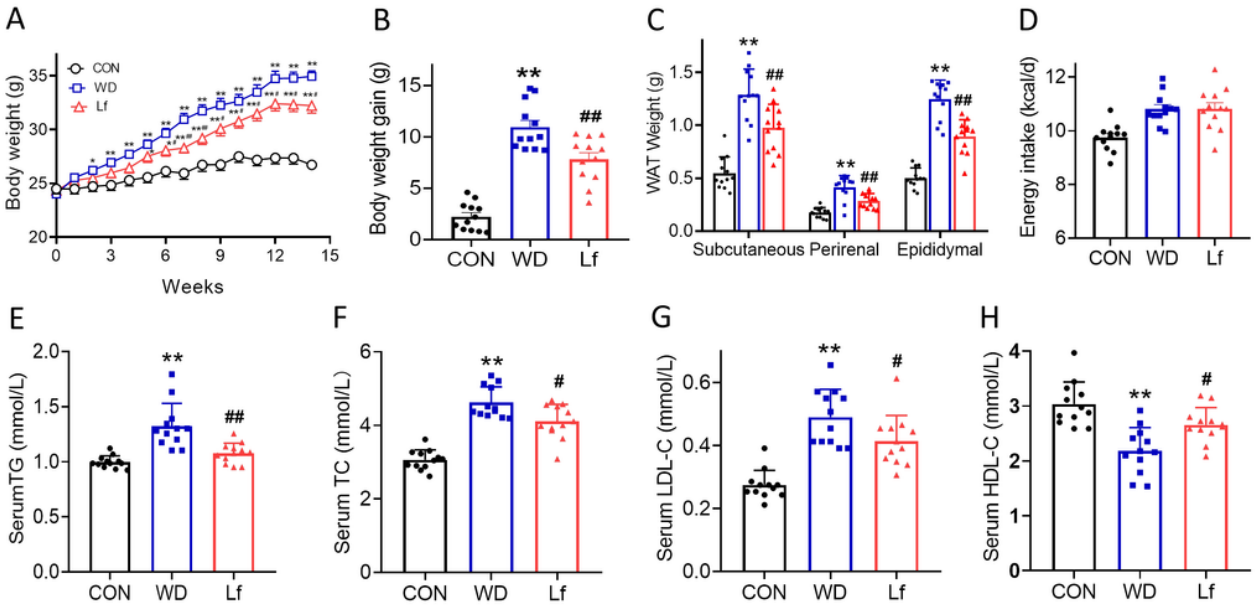

Figure 1

Lf intervention decreased body weight and improved lipid profiles in mice fed with 'Western'-style diets (WD). A. body weight trend during the experiment; B. body weight gain at the end of experiment; C. white adipose tissue (WAT) weight; D. energy intake; E-H. blood lipid profile. E. serum triglyceride (TG); F. serum total cholesterol (TC); G. serum low-density lipoprotein cholesterol (LDL-C); H. serum high-density lipoprotein cholesterol (HDL-C). n = 12 mice each group. *P < 0.05 vs. the CON group; **P < 0.01vs. the CON group. $^{\#}$P < 0.05 vs., the WD group; $^{\#\#}$P < 0.01 vs. the WD group.

Fig. 2

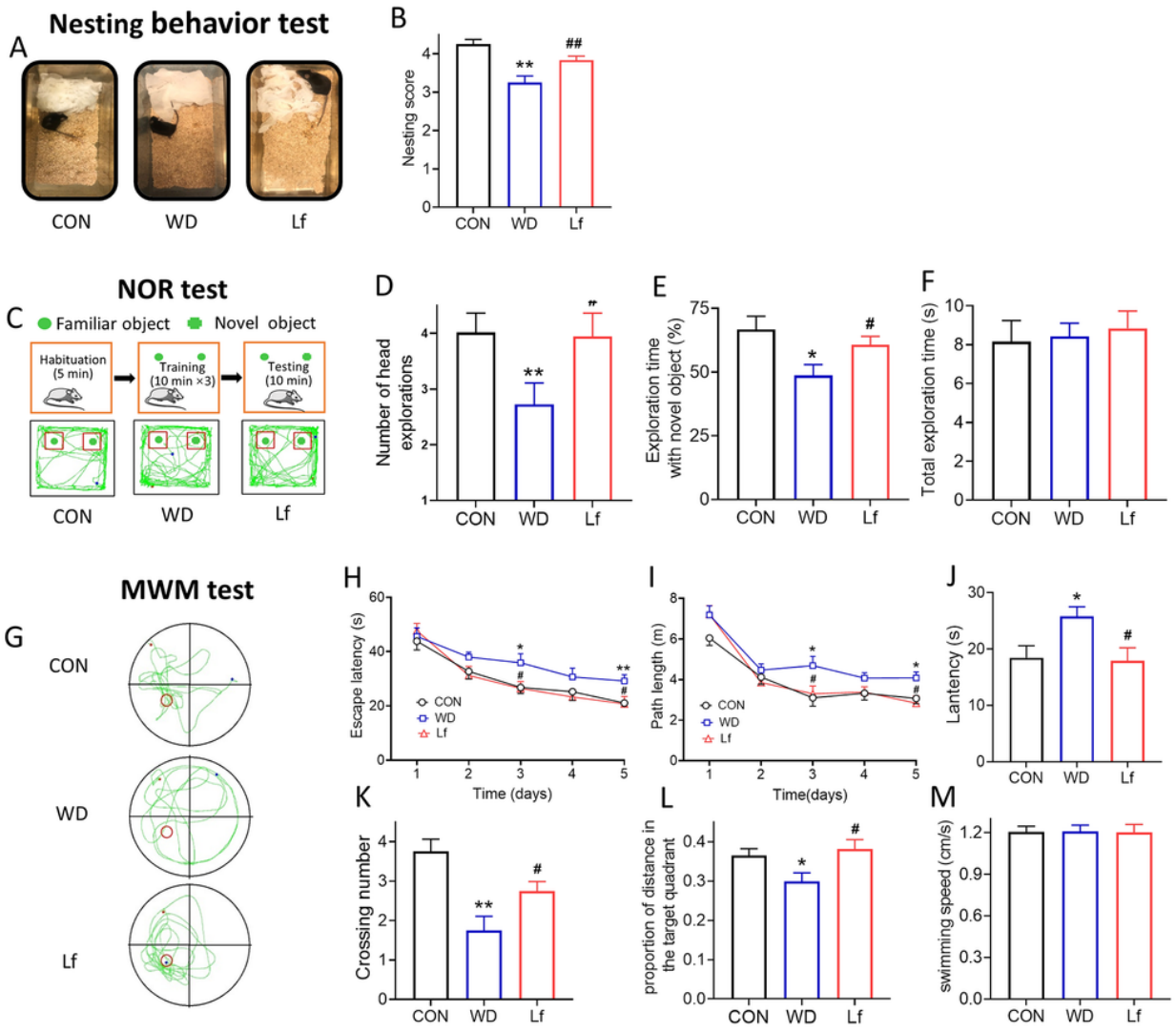

Figure 2

Lf intervention ameliorated 'Western'-style diets (WD)-induced cognitive impairment in mice. A, and B. nesting behavior test. A. pictures of test; B, the nest scores. C-F. novel object recognition (NOR) test. C. NOR diagram; D. percentage of time spent with the novel object to total object exploration time; E. the number of head explorations.; F. the total object exploration time; G-M. Morris water maze (MWM) test. G. trajectory diagram after removing the escape platform; H. escape latency; I. escape path length; J. escape latency after removing the escape platform; K. crossing number; L. proportion of distance in the target quadrant; M. swimming speed. n = 12 mice each group. *P < 0.05 vs. the CON group; **P < 0.01vs. the CON group. $^{\#}$P < 0.05 vs., the WD group; $^{\#\#}$P < 0.01 vs. the WD group.

Fig. 3

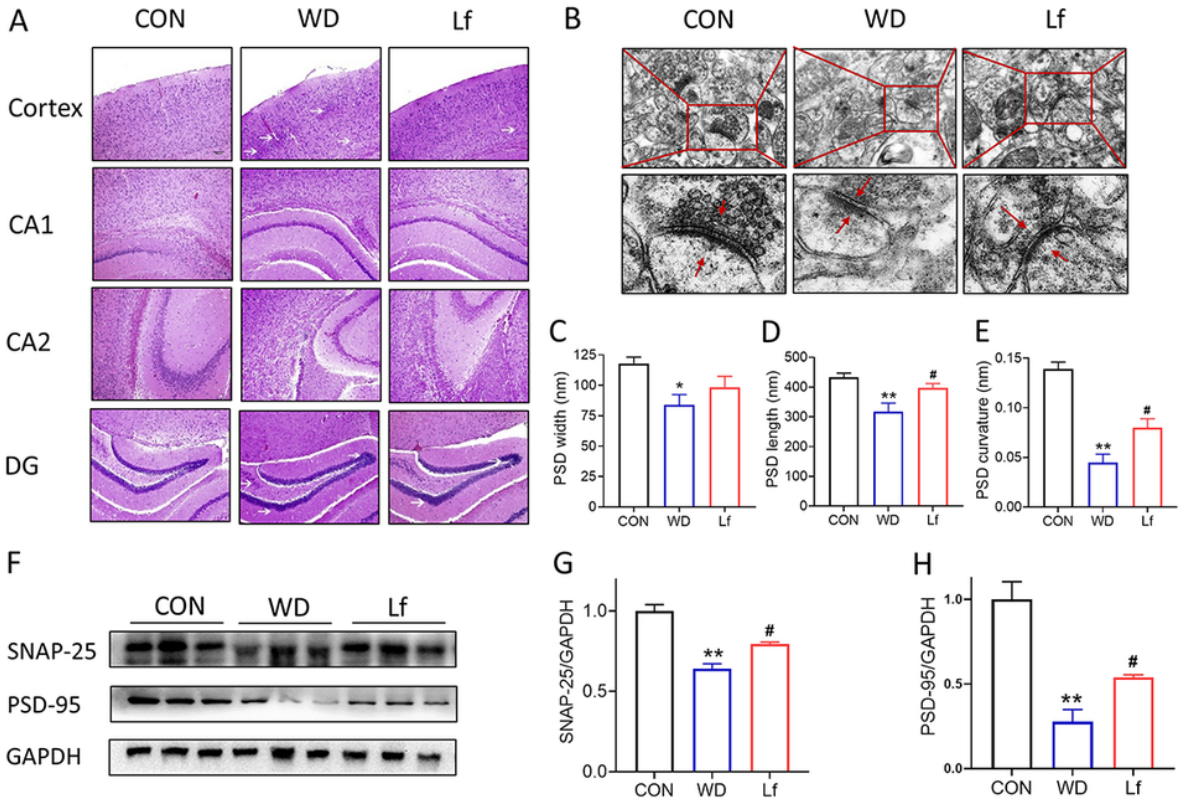

Figure 3

Lf intervention improved the hippocampal neurons and synapses in mice fed with 'Western'-style diets (WD). A. histopathology of mouse brain; B. representative image of ultrastructure of synapse in the hippocampus by transmission electron microscope (TEM); C. postsynaptic density proteins (PSD) width; D. PSD length; E) PSD curvature (n = 6 mice each group); F. representative western blots of synaptosomal associated proteins 25 (SNAP-25) and PSD-95.; G. quantitative measurement of SNAP-25; H. quantitative measurement of PSD-95 (n = 3 mice each group). *P < 0.05 vs. the CON group; **P < 0.01vs. the CON group. $^{\#}$P < 0.05 vs., the WD group; $^{\#\#}$P < 0.01 vs. the WD group.

Fig. 4

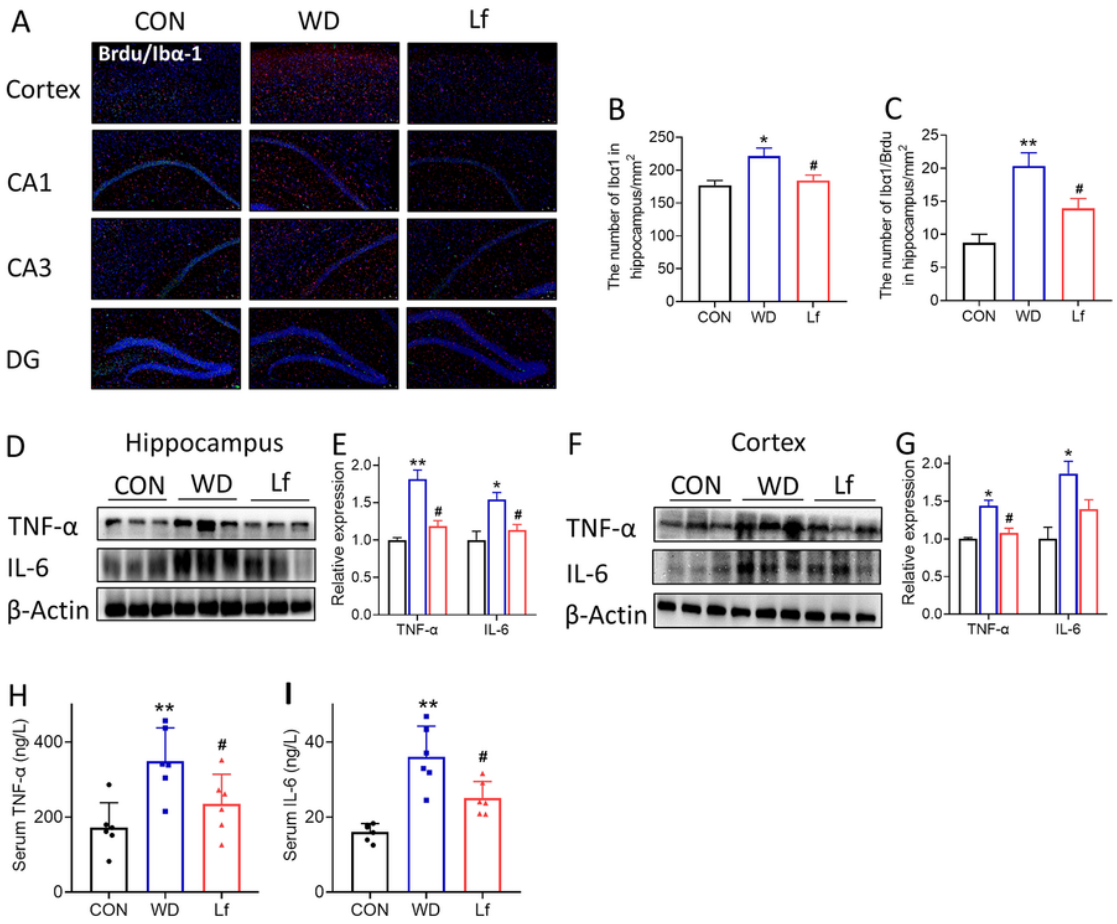

Figure 4

Lf intervention suppressed 'Western'-style diets (WD)-induced microglia activation and inflammation in the mouse brain and serum. A. representative immunofluorescence double staining of Ibα1 and BrdU; B. the number of Ibα1 in hippocampus; C. the number of Ibα1/Brdu in hippocampus. D. representative western blots of TNF-α and IL-6 in the hippocampus, and E. the quantitative measurement; F. representative western blots of TNF-α and IL-6 in the cortex, and G. their quantitative measurement (n = 3 mice each group); H. serum TNF-α; I. serum IL-6 (n = 6 mice each group). * $P < 0.05$ vs. the CON group; **$P < 0.01$vs. the CON group. $^{\#}P < 0.05$ vs., the WD group; $^{\#\#}P < 0.01$ vs. the WD group.

Fig. 5

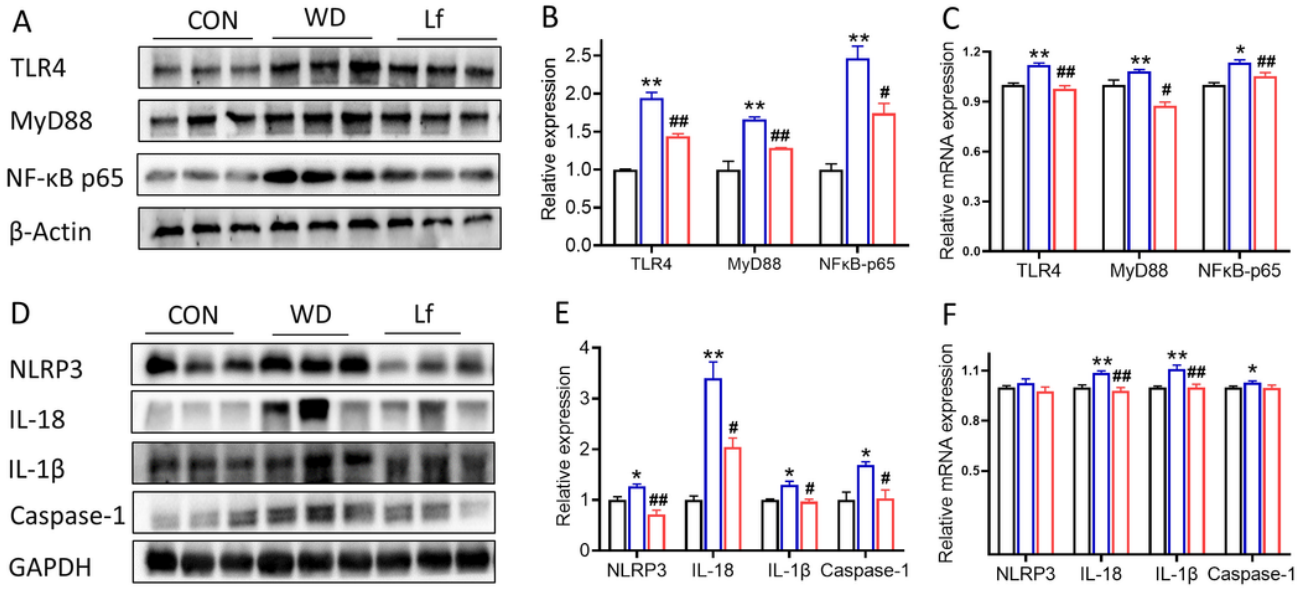

Figure 5

Lf intervention inhibited the 'Western'-style diets (WD)-induced activation of toll-like receptor 4 (TLR4)/nuclear factor kappa-B (NF-κB) signaling pathway and NOD-like receptor thermal protein domain associated protein 3 (NLRP3) inflammasomes in the mouse hippocampus. A. representative western blots of TLR4, MyD88 and NF-κB p65, and B. the quantitative measurement; C. the mRNA expression. D. representative western blots of NLRP3, IL-18, IL-1β and caspase-1, and E. quantitative measurement; F. the mRNA expression; (n = 3 mice each group). * $P < 0.05$ vs. the CON group; **$P < 0.01$vs. the CON group. $^{\#}P < 0.05$ vs., the WD group; $^{\#\#}P < 0.01$ vs. the WD group.

Fig. 6

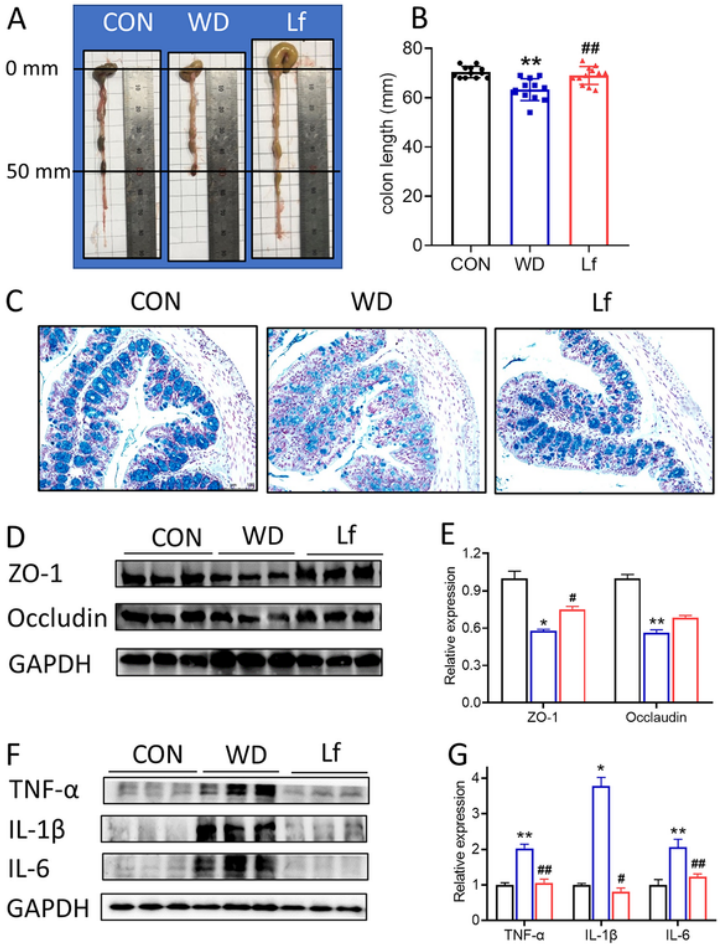

Figure 6

Lf intervention maintained colonic integrity and alleviated inflammation in mice fed with 'Western'-style diets (WD). A. representative images of colons, and B. the quantification of colon length; C. Alcian blue-stained colonic sections; D. representative western blots of ZO-1 and occludin in the mice colon, and E. quantitative measurement; F. representative western blots of TNF-α, IL-1β and IL-6 in the mice colon, and G. quantitative measurement (n = 3 mice each group). *P < 0.05 vs. the CON group; **P < 0.01vs. the CON group. $^{\#}$P < 0.05 vs., the WD group; $^{\#\#}$P < 0.01 vs. the WD group.

Fig. 7

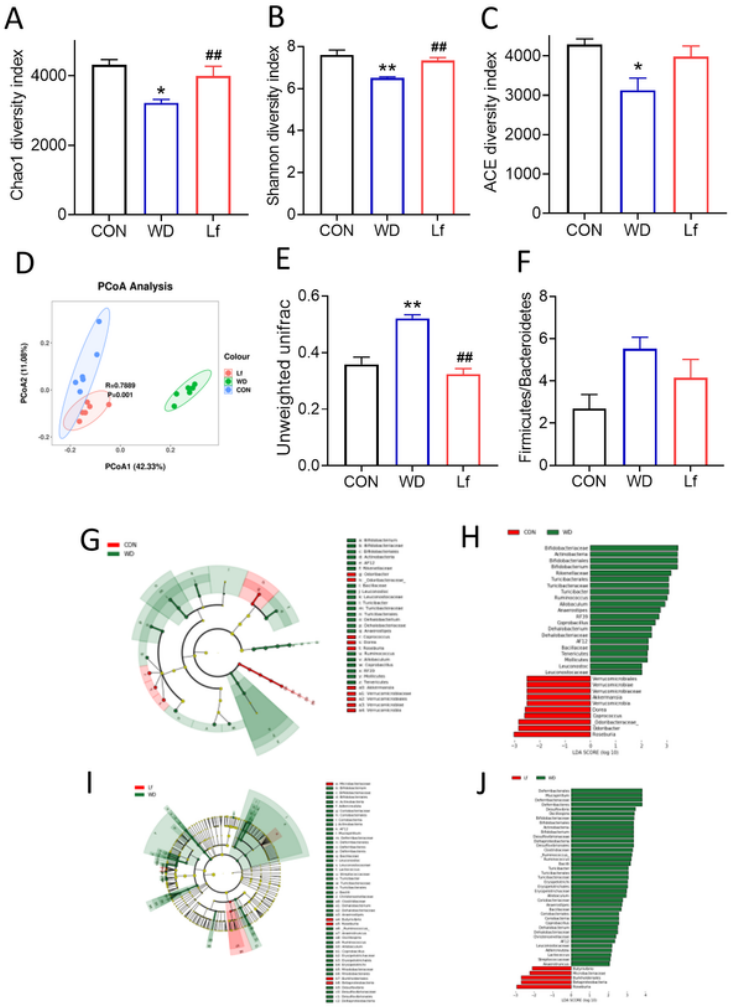

Figure 7

Lf intervention influenced gut microbiota alteration in mice fed with 'Western'-style diets (WD). A. Chao 1 diversity index; B. Shannon diversity index; C. abundance-based coverage estimator (ACE) diversity index; D. principal coordinates analysis (PCoA) based on unweighted UniFrac distances; E. unweighted uniFrac distances; F. the ratio of Proteobacteria/Bacteroidetes; G,H. linear discriminant analysis effect size (LEfSe) showing the most differentially significant abundant taxa enriched in microbiota from the CON and WD; I,J. LEfSe showing the most differentially significant abundant taxa enriched in microbiota from the Lf and WD (n = 6 mice each group); *P < 0.05 vs. the CON group; **P < 0.01vs. the CON group. $^{\#}$P < 0.05 vs., the WD group; $^{\#\#}$P < 0.01 vs. the WD group.

Fig. 8

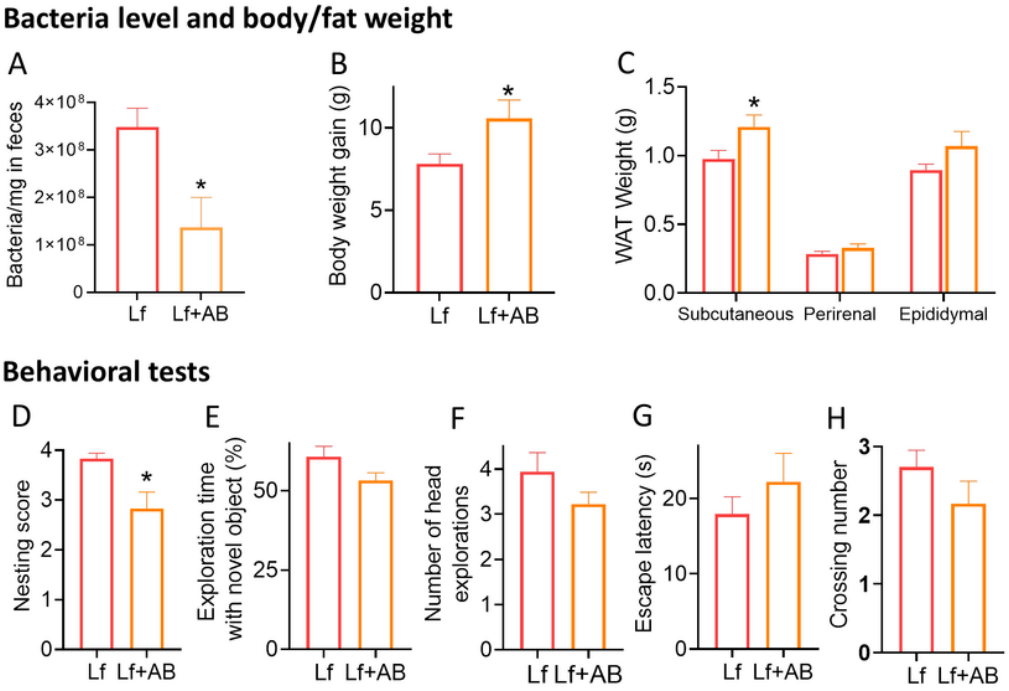

Figure 8

Antibiotics eliminated the effects of long-term Lf intervention in abrogating inflammation and cognitive impairment. A. bacteria level; B. body weight gain; C. WAT weight; D-H. behavioral tests. D. the nest scores in the nesting behavior test; E. percentage of time spent with the novel object, and F. the number of head explorations in the novel object recognition (NOR) test; G. escape latency, and H. crossing number in the Morris water maze (MWM) test. (n = 6 mice each group). *p < 0.05, **P < 0.01 vs. Lf group.

Fig. 9

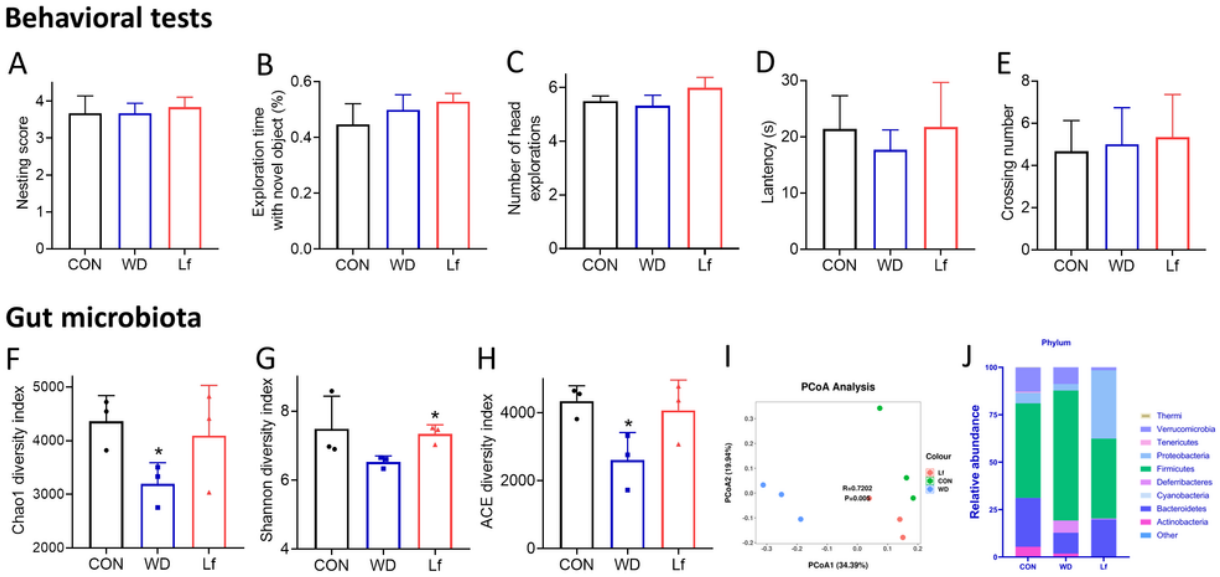

Figure 9

Lf intervention for 2 weeks prevented 'Western'-style diets (WD)-induced gut microbiota alteration prior to the behavioral cognitive changes. A. the nest scores in the nesting behavior test; B. percentage of time spent with the novel object, and C. the number of head explorations in the novel object recognition (NOR) test; D. escape latency, and E. crossing number in the Morris water maze (MWM) test. (n = 6 mice each group); F. Chao 1 diversity index; G. Shannon diversity index; H. ACE diversity index; I. PCoA based on unweighted UniFrac distances; J. relative abundance (n = 3 mice each group). *P < 0.05 vs. the CON group; **P < 0.01vs. the CON group. $^{\#}$P < 0.05 vs., the WD group; $^{\#\#}$P < 0.01 vs. the WD group.

Supplementary Files

This is a list of supplementary files associated with this preprint. Click to download.

- Fig.A1..tif
- Fig.A2..tif

- Graphabstract.tif
- TableA.1.DietIngredients.docx
- TableA.2.PairedprimersforqRTPCRanalysis.docx